THE EFFECT OF COOLING RATE ON THE MICROSTRUCTURE AND MECHANICAL PROPERTIES OF NICKEL ALUMINIUM BRONZE (NAB) ALLOY

BY

DOSUNMU, OLADIPO ANTHONY

MME/11/0424

A PROJECT REPORT SUBMITTED TO THE DEPARTMENT OF MATERIALS AND METALLURGICAL ENGINEERING

FACULTY OF ENGINEERING

FEDERAL UNIVERSITY, OYE-EKITI

EKITI STATE.

IN PARTIAL FULFILLMENT OF THE REQUIREMENTS FOR THE AWARD OF BACHELOR OF ENGINEERING (B.Eng) IN MATERIALS AND METALLURGICAL ENGINEERING

September, 2016

CERTIFICATION

I hereby certify that this project was carried out by **DOSUNMU, OLADIPO ANTHONY** with matriculation number ***MME/11/0424*** of the Department of Materials and Metallurgical Engineering, Federal University, Oye-Ekiti, Ekiti State, Nigeria and that this project has not been submitted elsewhere for a degree programme.

LADOL — 27/09/16

Student — Date

Bode Omotoyinbo — 16/2/17

Professor J.A. Omotoyinbo — Date

(Project supervisor)

21/2/17.

Professor A. Oni — Date

Head of Department

DEDICATION

I dedicate this research work to God Almighty for his immeasurable grace and mercy throughout the period of my Degree programme, and also to my parents and wonderful siblings for their encouragement, moral and financial support towards the success of the project.

ACKNOWLEDGEMENTS

My first gratitude goes to the impeccable God, the creator of the heaven and earth who has been faithful to me since the beginning of my programme and made this project a thing of reality. I express my thanks and appreciation to the HOD and all the staff of the department of Materials and Metallurgical Engineering.

I wish to express my profound gratitude and appreciation to my parents **MR AND MRS DOSUNMU**, my wonderful siblings and my project supervisor **Prof. J.A. OMOTOYINBO**. I consider myself fortunate to have had opportunity to work under his guidance and enrich myself from his vast knowledge.

I also express my thanks to the executives, workers, and every member of Redeemed Christian Fellowship, Fuoye Ikole Chapter. I sincerely appreciate all your encouragement, moral and spiritual support towards the success of this project.

I would also like to express my sincere gratitude to **Mr Akinfolarin, Mr Abel** for their immense assistance during the casting process.

Lastly, I want to appreciate my departmental friends **Olaleye John, Olugbemi Mayowa, Adegbenro Emmanuel**, to name a few, for their support all through my academic program and a very big thanks to my closest friend **Ariyo, Omokehinde Abisola** for her support morally, emotionally, financially and in prayers during the course of my project and academic program. God bless you all

ABSTRACT

This work studied the effect of cooling rate on the microstructure and mechanical properties of Nickel Aluminium Bronze (NAB) alloy. In this study, four different cooling media (air, oil, ice, fan) were employed during the cooling process of the cast nab.

The cooling in different media was carried out in order to assess their influence on its microstructure and mechanical properties.

Sand casting was used and was found to be effective based on its advantages of low cost, ease of use, flexibility, and availability of materials in the production of the nab alloy.

Microstructural analysis was also carried out on the cooled NAB alloys. The tensile strength and hardness of the various samples were also carried out. The result showed that the sample cooled with the use of a fan has the highest hardness and the sample cooled in spent engine oil has the highest tensile strength.

Keywords: NAB, MICROSTRUCTURE, HARDNESS, TENSILE TEST, SAND CASTING.

TABLE OF CONTENTS

CERTIFICATION.....i

DEDICATION.....ii

ACKNOWLEDGEMENTS.....iii

LIST OF FIGURES.....iv

LIST OF TABLES.....iv

LIST OF PLATES.....iv

ABSTRACT.....v

CHAPTER ONE

1.0 INTRODUCTION.....1

1.1 Background study.....1

1.2 Aim of study.....4

1.3 Objectives of study.....4

1.4 Scope of study.....4

CHAPTER TWO

2.0 LITERATURE REVIEW.....5

2.1 EFFECT OF COOLING ON NICKEL ALUMINUM BRONZE ALLOY....5

2.2 NICKEL ALUMINIUM BRONZE.....9

2.2.1 ALLOY ATTRIBUTES.....10

2.2.2 TYPICAL APPLICATIONS OF NAB ALLOY.....11

2.2.2.1 Marine Application.....12

2.2.3 NICKEL ALUMINUM BRONZE ALLOY PHASES.....14

2.2.3.1 Beta (β) and Retained-Beta (β') Phases.....14

2.2.3.2 Alpha (α) phase.....16

2.2.3.3 Kappa phases (κ).....16

2.2.4 NICKEL ALUMINUM BRONZE MICROSTRUCTURE.....18

2.3 MECHANICAL PROPERTIES.....19

2.3.1 Tensile Strength and Tensile Stress.....20

2.3.2 Compression test.....20

2.4 MECHANICAL PROPERTIES OF NICKEL ALUMINUM BRONZE ALLOY...21

2.4.1 Tensile strength.....23

2.4.2. Yield (Proof) Strength.....24

2.4.3. Hardness.....24

2.4.4. Ductility.....24

2.4.5. Wear resistance.....24

2.4.6. Shock resistance.....25

2.4.7. Fatigue strength.....25

2.4.8. Damping capacity.....25

2.4.9. Magnetic permeability.....25

2.5. Non-sparking characteristics.....26

2.5.1. Corrosion resistance.....26

3.0 METHODOLOGY.....27

3.1 Materials and Equipment.....27

3.2 ALLOY PREPARATION.....27

3.2.1. Sand moulding.....27

3.2.2. Melting.....28

3.2.3. Solidification of the alloy.....29

3.2.4. Finishing process.....30

3.3 MICROSTRUCTURAL EXAMINATION.....32

3.3.1. Specimen preparation.....32

3.3.2. Grinding and Polishing.....32

3.3.3. Etching.....33

3.3.4. Microscopic analysis.....34

3.4 HARDNESS TEST.....34

3.5 TENSILE TEST.....35

CHAPTER FOUR

4.0 EXPERIMENTAL RESULT AND DISCUSSION.....36

4.1 CASTING.....36

4.2. HARDNESS.....37

4.3. TENSILE STRENGTH.....38

4.4. MICROSTRUCTURE OF NICKEL ALUMINIUM BRONZE ALLOY....39

4.5. DISCUSSIONS OF THE MICROSTRUCTURES.....41

4.5.1 Microstructure of as-cast (air-sample) NAB alloy produced.....41

4.5.2 Microstructure of artificially cooled (fan) NAB alloy produced.....41

4.5.3. Microstructure of ice-cooled NAB alloy produced.....41

4.5.4. Microstructure of oil-cooled NAB alloy produced.....41

CHAPTER FIVE

5.0. CONCLUSION AND RECOMMENDATION.....42

5.1. CONCLUSION.....42

5.2. RECOMMENDATIONS.....43

REFERENCES.....44

LIST OF FIGURES

FIGURE 1A – SCHEMATIC MICROGRAPHS OF AS-CAST NAB.....6

FIGURE 1B – PHASE DIAGRAM OF CU-AL-5NI-5FE ALLOY.....6

FIGURE 2 – INITIAL MICROSTRUCTURE OF AS-CAST NAB.....8

FIGURE 2B – MICROSTRUCTURE OF AS-CAST NAB AFTER ANNEALING AT 675°C FOR 6 HOURS AND COOLING IN AIR.....8

FIGURE 3 – FSP AREA PROCESSING OF A MARINE PROPELLER.....13

FIGURE 4 – TRANSFORMATION PRODUCTS OF NAB DURING COOLING.....15

FIGURE 5 – EQUILIBRIUM TRANSFORMATION PRODUCTS OF COOLED CAST NAB.....18

FIGURE 6 – MICROSTRUCTURES CREATED IN NAB BY FSP.....19

FIGURE 7 – STRESS-STRAIN CURVE IN TENSION AND COMPRESSION.....21

FIGURE 8 – MECHANICAL PROPERTIES OF SELECTED ALLOYS.....22

FIGURE 9 – COMPARATIVE PRESSURE-TEMPERATURE RATINGS.....23

FIGURE 10 - SAND MOULD BOX USED FOR CASTING.....28

FIGURE 11 - CRUCIBLE FURNACE DURING MELTING PROCESS.....29

FIGURE 12 - PRODUCED ALLOY AFTER MELTING AND POURING.....30

FIGURE 13 - NAB ALLOY COOLING IN AMBIENT ATMOSPHERE.....31

FIGURE 14 - NAB ALLOY COOLING IN ARTIFICIAL ATMOSPHERE (FAN).....31

FIGURE 15 - NAB ALLOY COOLING IN SPENT ENGINE OIL.....31

FIGURE 16 - NAB ALLOY COOLING IN ICE BLOCK.....31

FIGURE 17 - GRINDING MACHINE.....33

FIGURE 18 - POLISHING MACHINE.....33

FIGURE 19 – POLISHED SAMPLE.....33

FIGURE 20 - OPTICAL METALLURGICAL MICROSCOPE.....34

FIGURE 21: NAB ALLOY TENSILE SPECIMENS.....35

FIGURE 22 - INSTRON UNIVERSAL TESTER (50KN) EQUIPPED WITH TENSILE JAWS.....35

FIGURE 23 - DIMENSIONS OF MACHINED NAB SAMPLE.....35

FIGURE 24 – TYPICAL MECHANICAL (HARDNESS) PROPERTY OF COOLED NAB SAMPLES.....37

FIGURE 25 – TYPICAL MECHANICAL (TENSILE STRENGTH) PROPERTY OF COOLED NAB SAMPLES.....38

LIST OF TABLES

TABLE 1 – COMPOSITION DATA (wt%) for NAB.....12

TABLE 2 – COMPOSITIONS OF PHASES PRESENT IN NAB (wt%).....17

TABLE 3 - CHEMICAL COMPOSITION OF NICKEL ALUMINIUM BRONZE (NAB) ALLOY AFTER CASTING (wt%).....36

TABLE 4 - HARDNESS OF THE COOLED NAB ALLOYS.....37

LIST OF PLATES

PLATE 1: MICROSTRUCTURE OF AS-CAST NAB ALLOY.....39

PLATE 2: MICROSTRUCTURE OF NAB ALLOY COOLED WITH FAN 39

PLATE 3: MICROSTRUCTURE OF NAB ALLOY COOLED WITH ICE BLOCK.....40

PLATE 4: MICROSTRUCTURE OF NAB ALLOY COOLED IN SPENT ENGINE OIL 40

CHAPTER ONE

1.0 INTRODUCTION

1.1 Background study

Nickel-aluminum bronze (NAB) alloy is one kind of copper-aluminum alloys. Due to high strength and excellent corrosion resistance, this alloy is widely used for marine equipment such as propellers, pumps, valves, *etc.* (Hassan et al, 1982). Under normal casting conditions, the microstructure is composed of α phase, several intermetallic phases (κ_i, κ_{ii}, κ_{iii}, and κ_{iv}) and a retained β phase (β′ phase) (Jahanafrooz et al, 1982). Nakhaie *et al.* found that the anodic character of κ phase with tens of millivolt is higher than that of copper-rich α phase, which increases the galvanic corrosion resistance of NAB alloy. In addition, the NAB alloy is reported to be susceptible to crevice and selective phase corrosion (Wharton and Stokes, 2008). Recently, several techniques have been used to improve both the corrosion resistance and mechanical properties of cast NAB alloy, such as equal channel angular extrusion (ECAE) (Ghao and Cheng, 2008), laser surface melting (LSM) (Tang and Cheng, 2004), and friction surfacing (FS) (Hanke et al., 2011). Tang *et al.* reported that laser surface melting improved the corrosion resistance and erosion resistance of cast manganese-nickel-aluminum bronze due to the formation of a homogeneous and single phase microstructure. Hanke *et al.* found that FS could improve the cavitation erosion of NAB because fine grains and homogeneous microstructure are obtained during friction surfacing. Friction stir processing (FSP) is a solid state metal working technique which was developed based on the basic principle of friction stir welding (FSW) (Mishra and Ma, 2005). During the FSP process, the specimen undergoes intense plastic deformation at simultaneously-elevated temperature, resulting in the formation of fine and equiaxed recrystallized grains. This method has been widely used to localize microstructure modification

in wrought, powder metallurgy and cast materials due to its energy efficiency, being environmentally-friendly, and versatility (Nandan et al., 2008). Microstructural evolution and mechanical properties of FSP NAB alloy have been studied in many literatures. Swaminathan *et al.* found that the peak temperature in the stir zone during FSP was 92% to 97% of the melting point. At "low" temperature, NAB undergoes intense plastic deformation during FSP, leading to grain refinement and microstructure uniformity. According to the previous literature, the refined grains and homogeneous microstructure can improve the mechanical properties of the NAB alloy (Oh-ishi and Su, 2011). The corrosion resistance of FSP NAB alloy is also enhanced by the refined grains (Ni et al, 2010). Song *et al.* found that FSP NAB suffers less severe attack than the as-cast NAB because FSP reduces the Volta potential difference among all the constituent phases in as-cast NAB. Moreover, the retained β phase can be produced when cooled at a high cooling rate, which has a harmful effect on the corrosion properties due to its direct contact with the cathodic sites and its martensitic structure (Song et al.. 2014). Lenard *et al.* also reported that the NAB composed of more β′ phase could produce pit corrosion after long-time exposure to sea water. In the previous literature, β′ phase can be restrained by means of heat treatment (Anantapong et al., 2014). However, post heat treatment of FSP NAB alloy has yet rarely been studied.

The microstructure of the alloy consists of a Cu-rich solid solution known as α-phase and β′-phase or martensitic β-phase, surrounded by lamellar eutectoid phase and a series of intermetallic k phases (Hassan et al. 1985). Among the intermetallic compounds, KI phase is rosette shape which is rich in Fe, KII phase is smaller than k_i phase and form a dendritic rosette shape which distributed at the α/β boundaries, K_{iii} phase is lamellar shape and it forms at the boundary of K_i phase and is rich in Ni and K_{iv} phase is a fine Fe rich precipitations that forms in α phase

(Wharton et al. 2005). The complexity of the alloy with several intermetallic phases lead to a significant change in the development of the microstructures, which can result in extensive corrosion resistance in seawater. Results of salt spray test on corrosion behavior of the alloy indicated that corrosion resistance has been improved in the heat treatment sequences like aging, quenching, normalizing and annealing. Characterizing the microstructure showed that quenching transforms all β phase into β′ phase and aging results in precipitation of fine k phases. On the other hand, annealing has led to the transformation of β′ martensite into α and k phases (Chen, 2007). Microstructure of the bronze alloy suffered from cavitation corrosion in seawater showed that the alloy was corroded by selective corrosion at the interface between α phase and intermetallic K precipitates, however, K precipitate-free zones were not considerably corroded. Crevice corrosion of the copper-based alloy was often associated with the formation of a Cu-ion concentration cell and an accelerated attack at the exposed area adjacent to the crevice (Schussler, 1993).

1.2 Aim of study

The aim of this research is to determine the effect of cooling rate on the microstructure and mechanical properties of nickel aluminum bronze alloy.

1.3 Objectives of study

The specific objectives of this research are to;

a) Produce nickel aluminium bronze alloy of known composition.

b) Set up different cooling media for the alloy produced in (a)

c) Determine the mechanical properties of the cooled alloys in (b)

d) Examine the microstructure of the cooled alloys using optical metallurgical microscope.

1.4 Scope of study

a) To prepare casting of Nickel Aluminium Bronze alloy by using crucible furnace and to let it solidify in sand mould.

b) To cool the solidified cast product in various cooling mediums.

c) To machine the cooled cast products and conduct tensile test.

d) To conduct hardness test on the cooled samples.

e) To study and analyze the microstructure of the cooled Nickel Aluminium Bronze alloy by using optical microscope (OM)

CHAPTER TWO

2.0 LITERATURE REVIEW

2.1 EFFECT OF COOLING ON NICKEL ALUMINUM BRONZE ALLOY

Nickel Aluminum Bronze (NAB) alloys have been used for various marine parts in seawater for many years. This alloy is a copper-based alloy including the main alloying; namely, nickel, aluminum and iron. Thus, NAB is an aluminum bronze, which has been further developed by adding about 5% nickel and 5% iron. The advantageous properties of the NAB are high strength and good corrosion resistance, especially when using in seawater condition (Dawson and Callcut, 1989). The key of the superior properties is a kappa (κ) structure containing high amounts of aluminum. From the results of former works (Robert and Thomas, 1982), casted NAB principally showed the intermetallic κ-phase structure, which could exist in many morphology characteristics; namely, K_i-phase that is similar to a rose or rosette, K_{ii}- phase having a globular grain, K_{iii}-phase in a lamellar form and K_{iv}-phase as fine precipitate. The coexistence of these κ-structures in NAB alloy depends on the composition of iron, nickel and copper that are different in each type. Since K_{iii}-structure has a shape of long continuous band, it can cause prior damage due to its sensitivity to chemical reaction compared with the basic α- structure of the alloy (Robert and Thomas, 1982). It was also found that when placing an object on a NAB sample containing small crevice on its surface, after soaking in seawater for about 1 month the area adjacent to the crevice was severely corroded. Corrosion depth of about 80 μm was especially observed next to the K_{iii}-phase (Robert and Thomas, 1982). Hence, it was recommended to avoid obtaining K_{iii}-phase in as-cast NAB alloy. Generally, microstructure of as-cast NAB is sensitive to corrosion due to the de-alloying. Thus, heat treatment process must be carried out subsequently after casting NAB alloy in order to adjust the κ- structure. The temperature, which

has been proved to be suitable for the heat treatment, is 675°C, at which formation of precipitates with high density in the matrix microstructure of NAB is provided (Hassan et al.,1982). The as-cast NAB microstructure basically consists of a copper-rich α (FCC) matrix, β (BCC) martensitic, Fe3Al and NiAl in form of intermetallic κ-phases, as illustrated in Fig. 1a (Hassan et al.,1982).

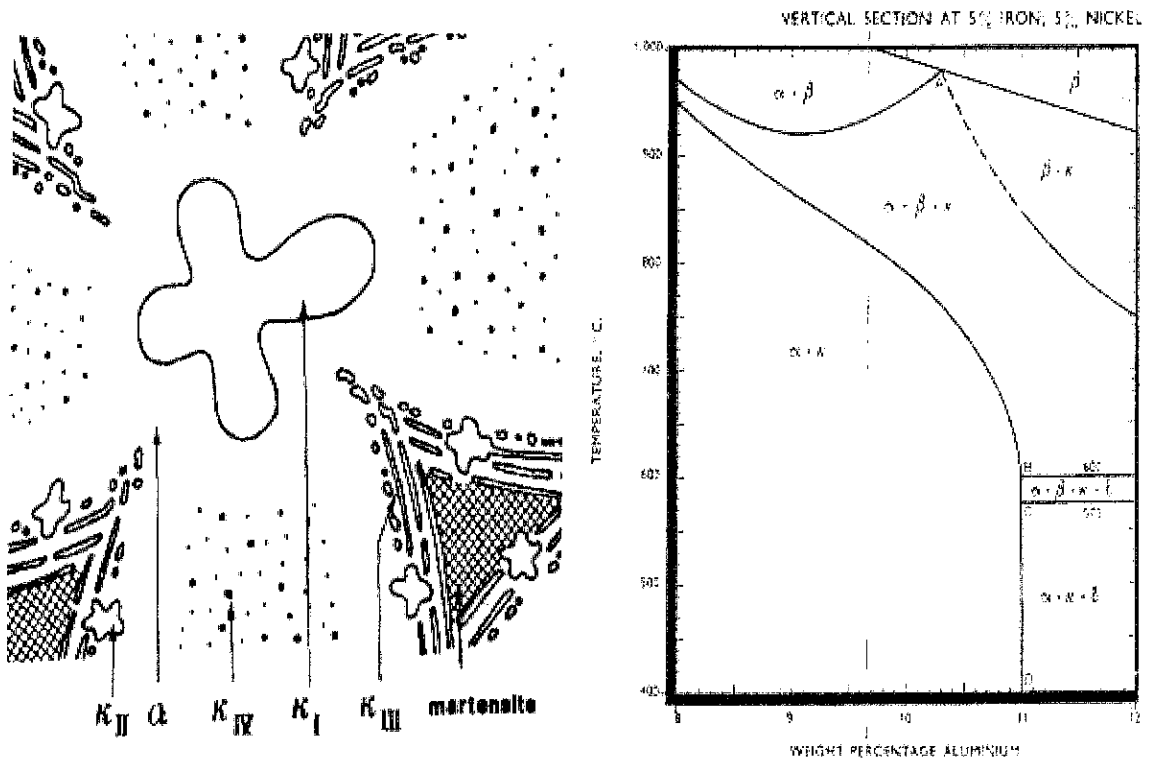

Figure 1 a) Schematic micrographs of as-cast NAB b) Phase diagram of Cu-Al-5Ni-5Fe alloy (Hassan et al.1982)

During slowly cooling down from casting temperature, the NAB alloy undergoes different microstructure changes, which can be seen in an equilibrium phase diagram in Fig. 1(b). At high temperature the microstructure composes of α and β phase. BCC β phase, which do not undergo diffusion decomposition by cooling, transforms into a complex martensitic structure containing a

high density of NiAl precipitates (Hassan et al.,1982). During cooling the β-phase transforms into the α-phase and κ-phases depending on the cooling rate. When the cooling rate is high, some β-phases may remain in the final microstructure. The development of the K_i-phase is very sensitive to alloy content and cooling rate. The K_{ii}-phase nucleates in the β phase and is occasionally found in the areas containing the K_{iii}-phase. While α- phase is growing, it envelops some K_{ii}-phases, which had formed at the α/β interface (Nelson, 2009). In previous studies of the Royal Thai Navy Dockyard (Thuanboon, 2010), a type of NAB alloy was produced using an open-die casting process. When considering the phase diagram of NAB alloy containing aluminum in the range of 8-11%, the results showed that the NAB microstructure consisted of a mixture of β phase and α phase embedded with intermetallic κ-phases at the temperature of 900°C. At the temperature lower than 900°C, the main structure changes from β phase to α phase including several types of intermetallic κ-phases. Fig. 2a presents typical microstructure of an as-cast NAB alloy. When the NAB specimen was annealed at 675°C for 6 hours and subsequently cooled in air, the microstructure was changed, as shown in Fig. 2b. It was observed that after heat treatment process no β phase remained in the microstructure. The altered microstructure mostly contained α phase and different types of K-phase, by which grain of the α phase became larger and κ-structure significantly increased.

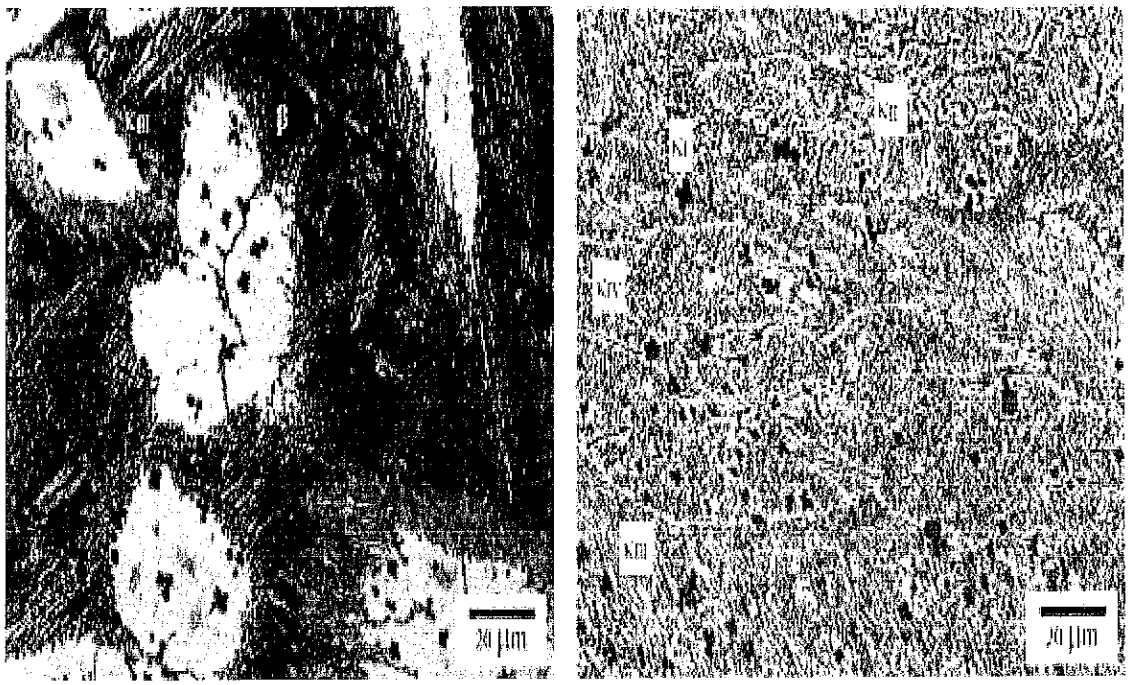

(a) (b)

Figure 2 a) Initial microstructure of as-cast NAB b) microstructure of as-cast NAB after annealing at 675°C for 6 hours and cooling in air (Thuanboon, 2010)

Recently, the effects of heat treatment parameters such as temperature, holding time and cooling rate on mechanical properties and microstructure evolution of as-cast aluminum based alloys were investigated (Ajeel et al., 2007). In forging process, working temperature shows considerable influences on the grain size of final workpiece of aluminum alloy. Thus, forming temperature is an important factor affecting the mechanical properties of the forged parts (Shan et al., 1997). It was found that for aluminum 7075 an optimum forging condition is to control the mold and specimen temperature to be around 460°C during the hot forming process (Weronski and Gontarz, 2003). For part having more complex shape, isothermal precision forging technology is normally used (Weronski and Gontarz, 2003). Hereby, the product quality can be adjusted as the requirements. Coarse grain structure occurred in hot forming process is

principally identified as material defect. This coarse grain structure leads to a strength deterioration of the produced parts (Shan et al., 1997). It was found that grain size of AlMgSi alloy was larger after forging when heating time was increased (Weronski and Gontarz, 2003). However, by higher forging force, grain size became smaller. To obtain a specific microstructure of the AlMgSi alloy, it is necessary to understand the effects of heating rate, forming temperature and loading level. For producing part from NAB alloy, there still has been a lack of such knowledge. The aim of this study was to investigate stress-strain behavior at high temperatures of a NAB alloy. The deformation temperatures of 825°C, 850°C and 900°C were considered. Note that these deformation temperatures were selected to be above the recrystallization temperature of the alloy. For the investigated NAB alloy, the melting temperature (Tm) was 1060°C and the recrystallization temperature was assumed to be 0.66Tm or about 707°C. The compression tests at constant strain rate were carried out for different isothermal temperatures. The stress-strain responses of the material were characterized. Consequently, the effects of temperature on the resulted microstructures, grain size and hardness of specimens after hot deformation were examined.

2.2 NICKEL ALUMINIUM BRONZE

Nickel aluminium bronze (NAB) alloy contain 10%Al, 5%Fe, and 5%Ni as the alloying elements. It has a density of 7.50g/cc and a magnetic permeability of 1.5 relative to air. It is widely used as engineering parts, such as various worm-gears, gears, bearings, dies, valves and propellers. The chemical composition of Nickel aluminium bronze are 78%Cu, 10% to 11.5%Al, 3% to 5%Fe, 3.5Mn max, 3.0% to 5.5% Ni, 0.5%max. This alloy type is fully weldable.

Nickel aluminium bronze alloy are generally two-phase, duplex alloys containing 5% - 10% aluminium as well as additions of iron and nickel for strength. Increasing the aluminium

content results in higher strength, which is attributable to a hard-body centered cubic phase which enhances properties of castings as well as hot working in wrought alloys. The other alloying elements also improve properties and alter microstructure. Specifically, Nickel improves corrosion resistance. While iron acts as a grain refiner and increases tensile strength. Nickel also raises yield strength and both nickel and manganese acts as microstructure stabilizer (Duma, 1975)

Nickel aluminium bronze are metallurgically complex alloys in small variations in composition can result in the development of markedly different microstructures, which can in turn result to wider variations in seawater corrosion resistance. Those microstructures, which result in optimum corrosion resistance, are obtained by control of composition and heat treatment.

2.2.1 ALLOY ATTRIBUTES

Nickel aluminium bronze alloy has various attributes which consist of their mechanical, thermal and physical properties which make them suitable for many applications. The alloy attributes are;

1. High hardness and wear resistance, providing excellent bearing properties in arduous applications.
2. Ductility, which like that for all copper alloys is not diminished at low temperatures.
3. Good weldability, making fabrication economical.
4. Readily machined, when compared with other high-duty alloys.
5. Low magnetic susceptibility, useful for many special applications.
6. Ready availability, in cast or wrought forms.
7. High resistance to cavitation erosion.
8. Resistant to scaling up to 1000°CL.

9. Good damping properties.
10. Excellent strength, similar to that of low alloy steels.
11. Excellent corrosion resistance, especially in seawater and similar environments, where the alloys often outperform many stainless steels.
12. Favorable high temperature properties, for short or long term range.
13. Good resistance to fatigue, ensuring a long service life.
14. Good resistance to creep, making the alloys useful at elevated temperatures.
15. Useful thermal conductivity.
16. Good bearing properties.
17. Oxidation resistance, for exposure at elevated temperatures and in oxidizing environments.
18. Ease of casting and fabrication, when compared to many materials used for similar purposes.
19. High resistance to cavitation erosion.

2.2.2 TYPICAL APPLICATIONS OF NAB ALLOY

Nickel aluminium bronze alloy possess many mechanical, thermal and physical properties suitable for many applications. The applications are;

a. **Industrial:** corrosion resistant articles, bushings, bearings, heat exchanger, flanges, tanks, structural members, pump shafts, aircraft part, plunger tips, welded piping systems, gears, pump parts, condenser tube for power stations, valve seats.
b. **Marine:** propellers, belt, nuts, ship building, marine hardware.
c. **Fasteners:** stuffing box nuts.
d. **Electrical:** electrical hardware.

e. **Consumer:** musical instruments, piano keys.

f. **Building:** window hardware.

g. **Plumbing:** facets

2.2.2.1 Marine Application

The use of certain compositions of Nickel Aluminum Bronze (NAB) for marine applications have earned it the nickname 'propeller bronze' (Sahoo, 1982). It exhibits a unique combination of properties including moderate strength and toughness, and excellent fatigue, corrosion, cavitation, and erosion resistance, which make it an outstanding choice of material for use as naval propellers (Wenschot, Sahoo and Culpan, 1987). These bronzes are Copper based alloys with additions of Aluminum, Nickel, Iron, and Manganese. The specification ASTM B 148-78 designation C95800 prescribes the nominal values for each of the alloy additions. Table 1 lists the nominal weight percentages of the alloying agents within propeller bronze as well as acceptable limits

Element	Cu	Al	Ni	Fe	Mn	Si	Pb
Min - Max	(min)79.0	8.5 – 9.5	4.0 – 5.0	3.5 – 4.5	0.8 – 1.5	0.10(max)	0.03(max)
Nominal	81	9	5	4	1	-	-

Table 1. Composition Data (wt%) for NAB. (ASTM B 148-78).

The problems associated with the use of this material often arise during manufacture. During fabrication, the ship propellers are cast in very large molds. The massively thick sections within the casting can take as long as a week to cool to ambient temperature. This corresponds to a very slow cooling rate on the order of 3 10 C s − ° for the thicker sections (Ohishi and McNelley, 2005). This slow cooling rate results in very coarse grains which confer poorer material

properties (Sahoo et al., 1979). On the other hand, the thinner sections of the casting experience a faster cooling rate (Wenschot, 1987). Due to the wide variation of cooling rates in the various thicknesses, the NAB microstructure sometimes exhibits segregation and gas evolution, resulting in porosity (Wenschot, 1987). This porosity creates additional difficulties in the fabrication process requiring fusion welding to fill in the pores, x-ray or ultrasonic inspection, grinding, and possible re-welding. This porosity repair can result in a repetitive cycle of repairs which can create propeller post-cast processing times up to 18 months. FSP is intended to replace the fusion weld repair cycle during the post-cast process. FSP can be used to selectively treat specific regions of the propeller's surface or the entire cast structure. FSP will surface harden the material and close any porosity defects near the surface layer of the propeller.

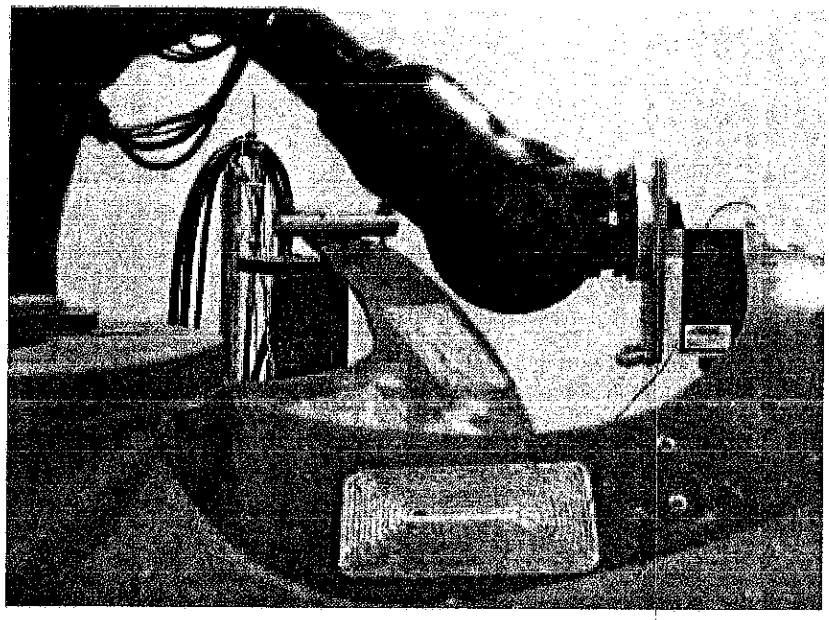

Figure 3. FSP Area Processing of a Marine Propeller, (Mahoney et al., 2003).

2.2.3 NICKEL ALUMINUM BRONZE ALLOY PHASES

FSP involves high temperatures, strains and strain rates, as well as a range of cooling rates. These parameters affect the microstructure of NAB and are responsible for its increase in material properties. There are four main phases that can form during the transformation of NAB and these transformation products greatly affect the material properties of the resulting microstructure (Ohishi and McNelley, 2005)

2.2.3.1 Beta (β) and Retained-Beta (β') Phases

The β phase is a high temperature solid solution phase of NAB. It is generated during the hot working process in FSP where temperatures exceed 1000°C. The β structure is BCC at high temperatures with a lattice parameter of 0.3568 nm (Hassan et al., 1982). This phase is not stable at ambient temperature; therefore, it must transform into various products as it cools. A variety of transformation products form as a function of cooling rate. Figure 4 outlines the transformations that result during cooling of NAB.

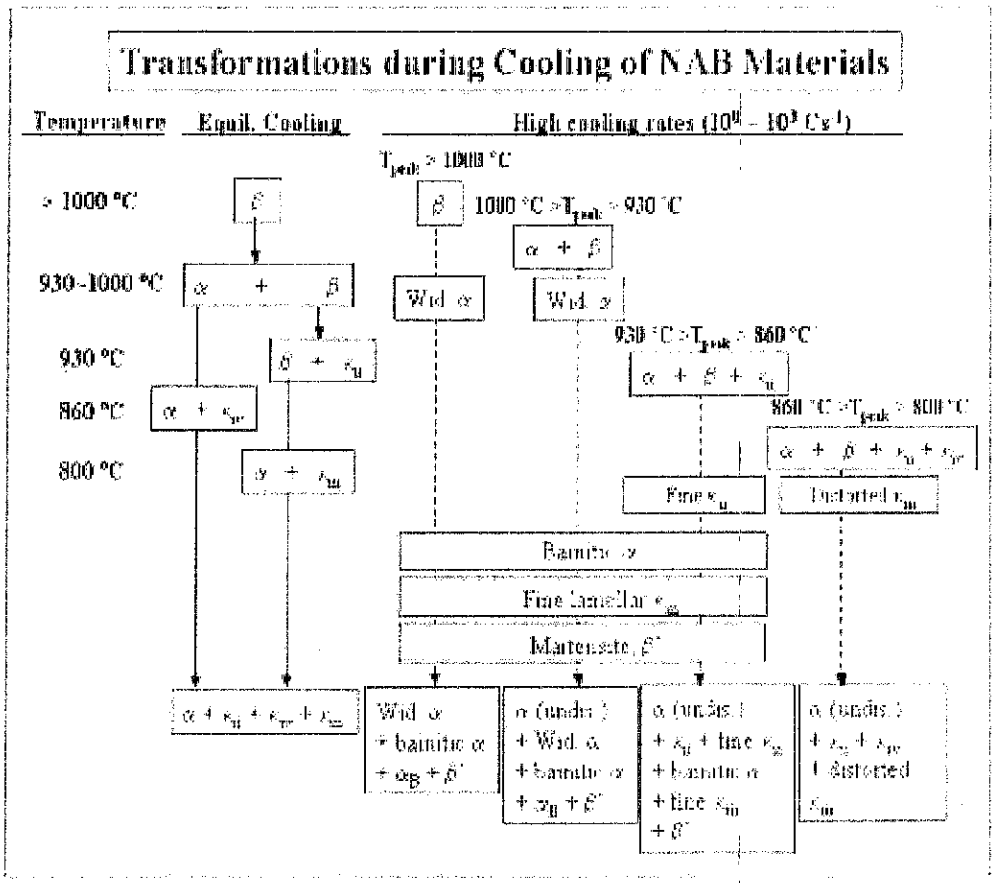

Figure 4. Transformation Products of NAB during Cooling, (Fuller 2006).

The left side of the figure is for equilibrium cooling, the same cooling which propeller castings are likely to encounter. The very slow cooling rate results in virtually all of the β transforming into alpha (α) and kappa (κ) products (Culpan and Rose, 1978). FSP results in considerably faster cooling rates and the material response is outlined in the right hand side of the Figure 4. Depending of the peak temperature attained in the FSP process, the microstructure will resolve into more complex component mixtures that include primary α and β transformation products. The latter structure includes α in a Widmanstatten morphology, β in coarser to finer bainite structures, or martensitic beta (β') (Culpan and Hassan, 1982). A high density of precipitates form throughout the β on cooling, acting as nucleation sites for the formation of primary α. The

β composition varies throughout the structure depending on the amount of alloying elements that are consumed while forming other phases or particles. In the optical micrographs included in this report, the dark etched constituent represents the various forms of β.

2.2.3.2 Alpha (α) phase

The α phase is the terminal solid solution constituent of NAB. The α structure is FCC at room temperatures with a lattice parameter of 0.364 nm (Hassan et. al., 1982). It is usually the first constituent to form upon cooling of β. The temperature at which α forms is dependent on composition (Culpan and Rose, 1978). The composition of the α phase varies during the cooling process as elements are transferred at the α / β interfaces and from within β to form additional phases.

2.2.3.3 Kappa phases (κ)

There are four distinct κ phases which form during the cooling of NAB. They form as a result of the decreasing solubility of iron, aluminum, and nickel during the cooling process (Culpan and Hassan, 1982). They are all stable at ambient temperatures. The first kappa phase (κ_i) is usually found in NAB compositions wherein the iron content is greater than 5%, and κ_i may begin forming in the melt (Hassan 1982). It is generally surrounded by the α phase. The κ_i precipitates are mostly iron rich (FeAl, Fe_3Al) and surround small copper rich particles. Its crystal structure varies between BCC, DO3, and B2 (Hassan 1982). When present, κ_i exhibits a large rosette shape, 20-50 microns in diameter, and will etch grey in a micrograph. This phase is not likely to be encountered in the NAB alloy which this report considers. The κ_{ii} phase is iron rich (Fe_3Al) and has a DO3 lattice structure (Hassan 1982). These particles begin to nucleate in the β near α / β interfaces. These particles are usually between 5-10 microns in diameter (Hassan 1982). These

particles tend to form at the same temperature as Widmanstatten α. The k_{iii} phase is the only phase that is nickel rich (NiAl). It has a B2 lattice structure (Hassan 1982). This phase forms upon cooling below 800°C. The NAB alloys with the highest nickel concentration tend to form the most κ_{iii}. This phase can take on a globular or lamellar form, but maybe difficult to observe in micrographs since some etching solutions preferentially attack this structure. The fourth kappa phase (κ_{iv}) has an inter-atom spacing and lattice structure similar to κ_{ii} . These particles are found distributed throughout the α grains, except in a precipitate free zone surrounding primary α grains. The nominal compositions of all the phases found in NAB after equilibrium cooling are listed in Table 2. Figure 5 is a micrograph showing α and κ transformation products of β during equilibrium cooling of cast NAB material.

Phase	Cu	Al	Ni	Fe	Mn
Alpha	85.4	8.3	2.5	2.7	1.4
Beta	85.2	8.7	3.5	1.6	1
Kappa I	8.4	17.5	3	65.6	2.7
Kappa II	9.3	22.2	6.6	53	1.9
Kappa III	12	44.3	31.5	10.2	1.6
Kappa IV	2	18.9	6.1	63.8	2.1

Table 2. Compositions of Phases Present in NAB, In Weight Percent, From (Hassan 1982).

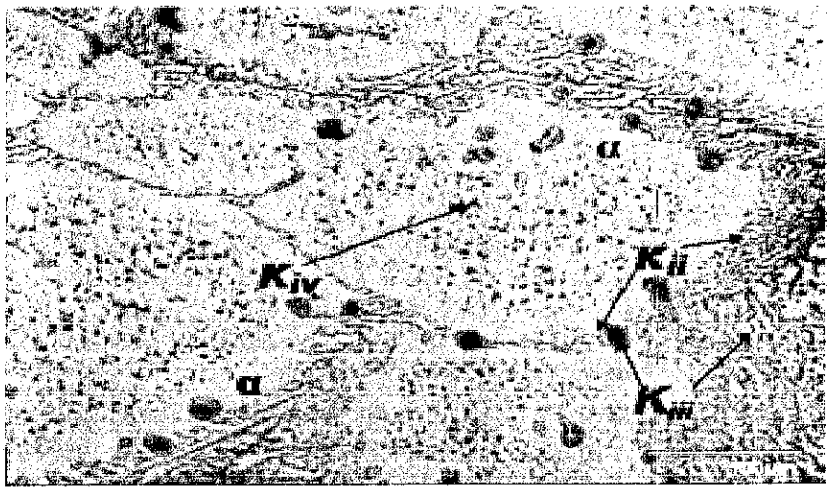

Figure 5. Equilibrium Transformation Products of Cooled Cast NAB, (Fuller, 2006).

2.2.4 NICKEL ALUMINUM BRONZE MICROSTRUCTURE

The above phases contribute to the formation of four primary microstructures associated with FSP of NAB material. The microstructures within and surrounding the stir zone are: a) lamellar, b) fine grain, c) Widmanstatten, and d) as-cast. Figure 6 is a composition of micrographs that show the three unique types of microstructures encountered in FSP (a-c) as well as a comparison (d) microstructure of as-cast NAB material.

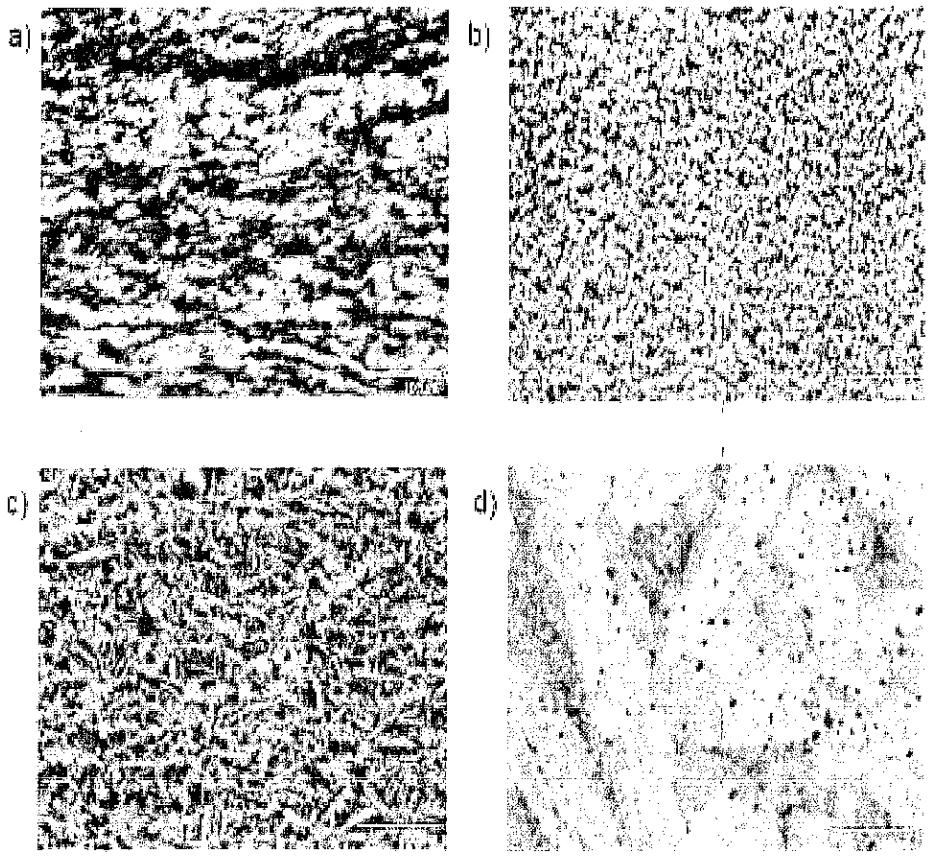

Figure 6. Microstructures created in NAB by FSP, (Fuller, 2006).

2.3 MECHANICAL PROPERTIES

The mechanical properties are about the behavior of materials when subjected to forces. When a material is subjected to external forces, the internal forces are set up in the materials which oppose the external forces. The material can be considered to be rather like a spring. Spring, when stretched by external forces, sets up internal opposite forces which are readily apparent when the spring is released and the force is to contract. A material subjected to external forces which stretch said to be in tensile force. A material subject to force which squeezes is referred to as compressive force.

2.3.1 Tensile Strength and Tensile Stress

Perhaps the most natural test of a material's mechanical properties is the tension test, in which a strip or cylinder of the material, having length L and cross-sectional area A, is anchored at one end and subjected to an axial load P – a load acting along the specimen's long axis – at the other. As the load is increased gradually, the axial deflection δ of the loaded end will increase also. Eventually the test specimen breaks or does something else catastrophic, often fracturing suddenly into two or more pieces. As engineers, we naturally want to understand such matters as how δ is related to P, and what ultimate fracture load we might expect in a specimen of different size than the original one. As materials technologists, we wish to understand how these relationships are influenced by the constitution and microstructure of the material.

When reporting the strength of materials loaded in tension, it is customary to account for the effect of area by dividing the breaking load by the cross-sectional area:

$$\sigma_f = \frac{P_f}{A_0} \qquad (1.1)$$

where σ_f is the ultimate tensile stress, often abbreviated as UTS, Pf is the load at fracture, and A_0 is the original cross-sectional area.

2.3.2 Compression test

The above discussion is concerned primarily with simple tension, i.e. uniaxial loading that increases the interatomic spacing. However, as long as the loads are sufficiently small (stresses less than the proportional limit), in many materials the relations outlined above apply equally well if loads are placed so as to put the specimen in compression rather than tension. The expression for deformation and a given load,

$$\delta = \frac{P L}{AE} \qquad (1.2)$$

It applies just as in tension, with negative values for δ and P indicating compression. Further, the modulus E is the same in tension and compression to a good approximation. The stress-strain curve simply extends as a straight line into the third quadrant as shown in Figure 7.

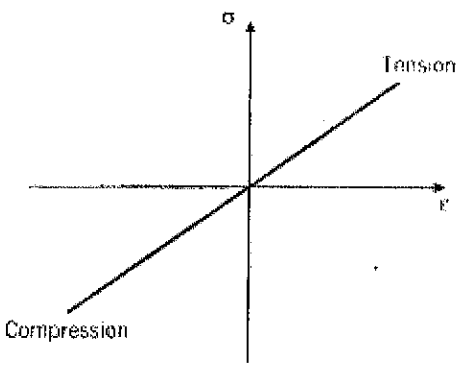

Figure 7. Stress-strain curve in tension and compression.

There are some practical difficulties in performing stress-strain tests in compression. If excessively large loads are mistakenly applied in a tensile test, perhaps by wrong settings on the testing machine, the specimen simply breaks and the test must be repeated with a new specimen.

2.4 MECHANICAL PROPERTIES OF NICKEL ALUMINUM BRONZE ALLOY

Returning to the myth of NAB being weak: the tensile and yield strengths are shown graphically in Figure 8. This illustrates several points clearly. First, the difference between "bronze" and NAB is significant and shows the association with bronze can damage the reputation of NAB. The yield strength of NAB is over double that of bronze (also known as gunmetal or valve bronze)

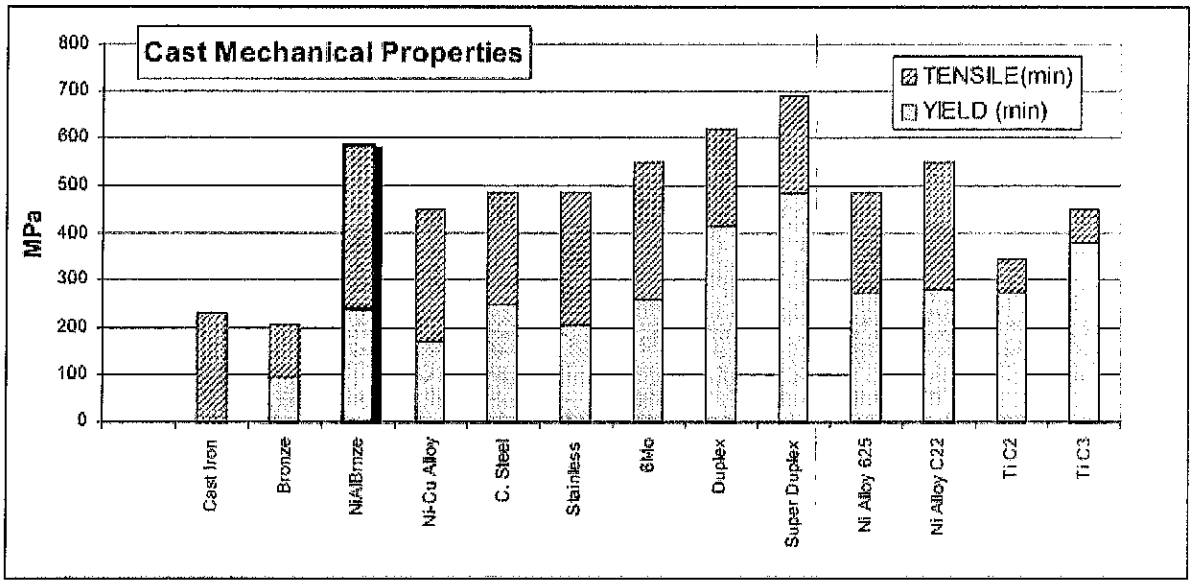

Figure 8. Mechanical properties of selected alloys (ASME B16.24-2006)

Second, perhaps more surprisingly, NAB's mechanical properties are better than those of Ni-Cu alloy. While there are high strength Ni-Cu wrought alloys such as K-500, the common cast alloys do not perform so well, as is illustrated (ASME B16.24-2006). Additionally, the common carbon and stainless steels materials do not differ significantly as far as these properties are concerned. The duplex and super-duplex materials are the only ones to significantly exceed the mechanical properties of NAB. Even the commonly used grades of titanium have an inferior performance to NAB. Although the ductility of NAB is not as high as most of the materials compared, it matches titanium and, with a 15% elongation, cannot be considered brittle (Blake, 2001).

For valves, the mechanical properties by themselves are not a determining factor. Variety is reduced and standardization is greatly assisted by adopting a philosophy of a standard set of dimensions with a pressure-temperature rating dependent on the material. This is based on material mechanical properties taking account of the performance at varying temperatures.

So when comparing materials, it is the pressure temperature rating that should be compared. Figure 9 shows the cold working pressure (CWP) for the various materials. The comparison is not straightforward because the bronze and cast iron figures relate only to flat-face flanges and all the other dimensions relate to the ANSI B16.5 raised face dimensions. Additionally, in the absence of appropriate standards, the NAB and titanium ratings have been specially calculated.

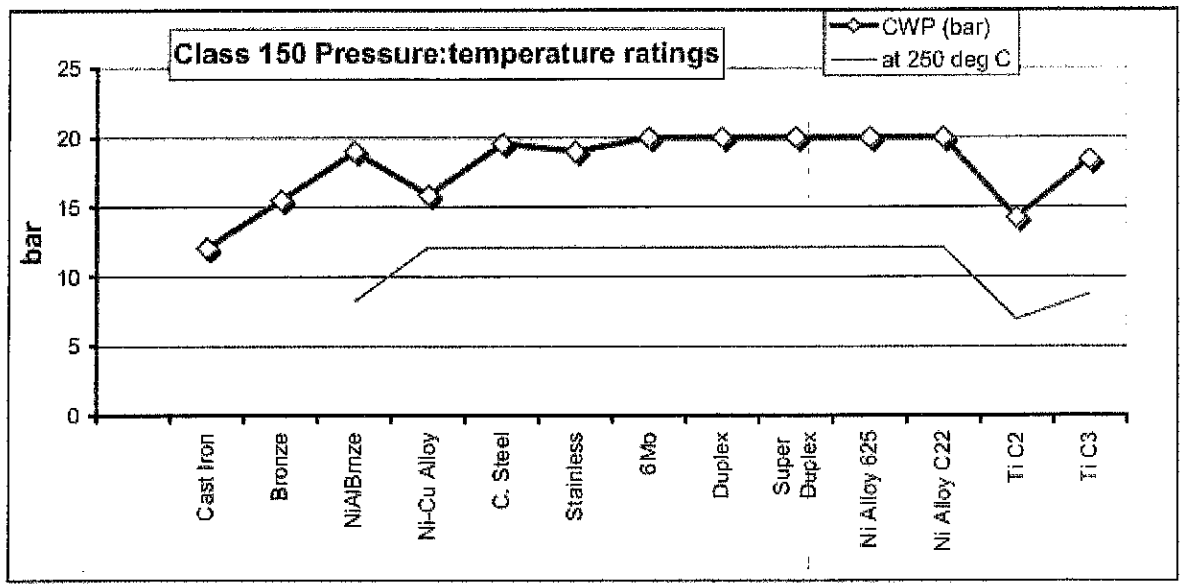

Figure 9. Comparative pressure - temperature ratings (ASTM B148-97(2003)

2.4.1 Tensile strength

Some aluminium bronzes exhibit strengths comparable to low alloy steels and many are stronger than most stainless steels. Furthermore, the alloys retain a substantial proportion of their strength at elevated temperatures, and at low temperatures, they gain strength slightly while retaining ductility. Shear strength can be estimated as being two-thirds of the tensile strength.

2.4.2. Yield (Proof) Strength

Yield (proof) strength is a more useful property than tensile strength since it is a measure of the stress needed to cause a measurable permanent (non-elastic) deformation, i.e. far lower than the stress needed to cause failure. However, yield strength is not quite so easy to measure as is tensile strength in this case because, unlike steels, copper alloys do not show a sudden "yield" deformation is increased past a critical value, so "proof strength" is a more appropriate term.

2.4.3. Hardness

The hardness of aluminium bronzes increases with aluminium (and other alloys) content as well as with stresses caused through cold working. Some manganese and manganese nickel-aluminium bronzes exhibit martensitic transformations similar to those seen in steels, but while those reactions produce higher mechanical properties, they are not generally thought of as primary strengthening mechanism.

2.4.4. Ductility

Most aluminium bronzes show ample ductility to provide adequate service life and to resist fatigue. Again, values attainable vary with alloy content and amount of prior cold work. Elongation figures decrease as the alloys get harder.

2.4.5. Wear resistance

From the standpoint of wear resistance, aluminium bronzes often provide excellent service in both cast and wrought forms. Metal-sprayed or welded overlay deposits of aluminium bronze on steel also provide effective wear-resistant surfaces.at the high end of the wear and abrasion resistance spectrum are special aluminium bronze alloys containing up to 14% aluminium,

whose applications include dies for deep drawing and moulds for die casting, casting of glass bottles and pressing vinyl records. Such alloys are quite brittle and are exclusively used as overlays.

2.4.6. Shock resistance

Aluminium bronze alloys, and in particular the wrought products have excellent resistance to shock provided, as always, that the material is sound and undue stress concentrations are avoided in design.

2.4.7. Fatigue strength

Aluminium bronzes possess exceptional resistance to fatigue, which is one of the most common cause of deterioration in marine engineering equipment. This property helps to give the alloys their excellent resistance to corrosion fatigue that makes them suitable for use as propellers and in pumps.

2.4.8. Damping capacity

Aluminium bronzes are twice as effective as steel in their ability to dampen vibrations.

2.4.9. Magnetic permeability

Aluminium bronzes can be made with exceptionally low magnetic permeability and are therefore ideal for non-magnetic instrumentation, survey vessels, mine counter-measure craft and other marine parts where permeability must not exceed 1.05. The magnetic permeability of certain aluminium bronzes is often less than 1.01, whereas that of austenitic stainless steels can be higher than this value if excessive ferrite is present.

2.5. Non-sparking characteristics

Excellent non-sparking characteristics make Aluminium bronzes suitable for the manufacture of tools and equipment used in the handling of explosives, in mines, petroleum and chemical plants, gas-handling equipment and similar applications.

2.5.1. Corrosion resistance

Aluminium bronzes can be used in environments that are far more aggressive than are tolerated by most other metals, including even copper and the brasses used for general purposes. They can provide heavy-duty service at higher temperatures, in seawater environments and in the presence of many chemicals and acids. Much useful work has been to characterize the corrosion resistance of these alloys so that best use can be made of them.

Like many copper alloys, aluminium bronzes also resist bio-fouling in both fresh and saline waters. This property is useful in propellers and especially so in seawater piping. (*http://properties.copper.org/*)

CHAPTER THREE

3.0 METHODOLOGY

3.1 Materials and Equipment

a. Copper coils
b. Aluminium metal
c. Nickel metal
d. Weighing balance
e. Crucible furnace
f. Sand mixer
g. Cope and drag
h. Grinding and polishing machine
i. Hack saw
j. Metallurgical microscope
k. Instron universal tester (50KN)
l. Digital Rockwell tester

3.2 ALLOY PREPARATION

The preparation of the alloy was carried out in the foundry workshop. The first stage in the alloy preparation is the sand moulding.

3.2.1. Sand moulding: Sand is used to create the mould. The sand is typically silica sand mixed with a type of binder to help maintain the shape of the mould cavity. Typical composition of the mixture is 90% Silica sand, 3% water, and 7% clay or binder. The pattern is placed with the parting surface downward on the moulding board. The pattern is checked to see if the draft is

pointing upward, so that when the flask is turned, the pattern may be removed easily from the mould. The flask level is filled with unriddled, tempered sand from the floor which is then rammed uniformly around the outer edge of the flask. A gate is cut with a gate cutter from the mould cavity to the sprue hole. The cross-sectional area of the gate should be less than that of the sprue in order to flow clean metal into the mould.

The cope was carefully placed on the drag making sure that they are aligned properly. The molten metal can then be poured.

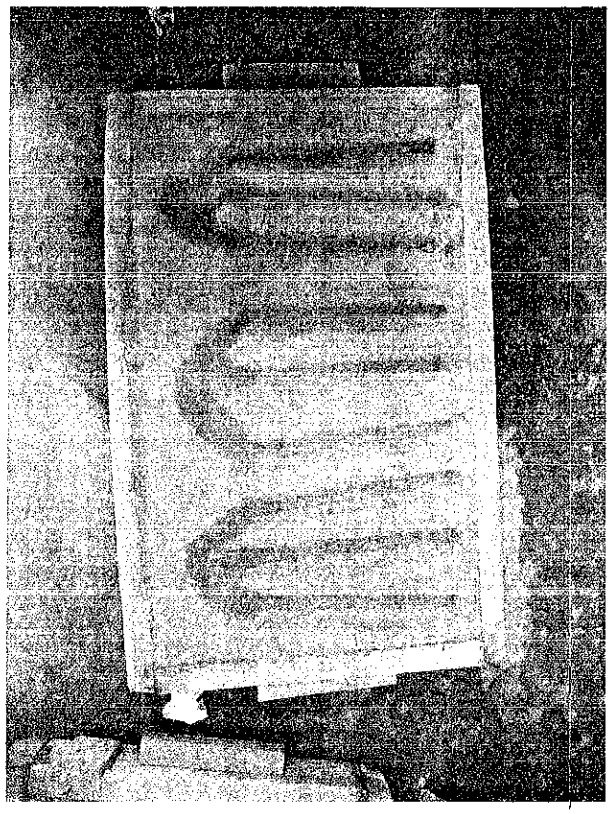

Figure 10. Sand mould box used for casting

3.2.2. Melting: Melting is basically a process of converting a metallic substance (the alloying elements) from its solid state into liquid state by heating them together above their melting point in the crucible furnace.

A crucible furnace is used in melting non-ferrous metals such as aluminium, brass, bronze, tin, lead and zinc. The process started with preparation of the charge containing required quantities of different elements (Cu, Ni, Al). The copper coils were charged in a crucible and melted in the furnace. The melt surface was covered with flux and the other alloying elements will be added to the melt (maintained at 1170°C) gradually.

Care was taken to add the lower melting elements like Al at latter stages of melting with a view to reduce losses through vaporization. The melt was stirred manually for some time to facilitate dissolution of the alloying elements. After cleaning the melt surface, pouring was carried out in moulds in the form of 20mm diameter, 200mm long cylindrical rods.

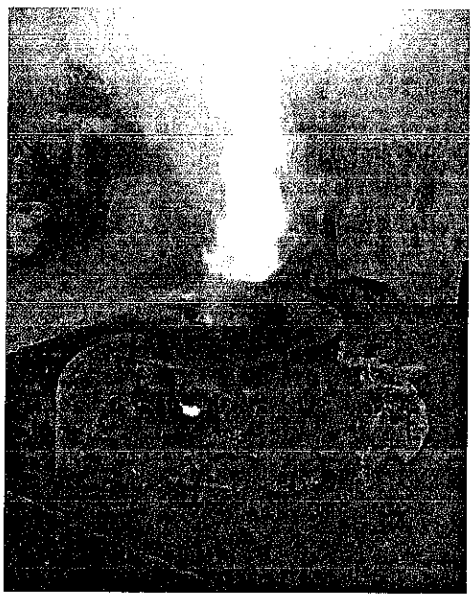

Figure 11. Crucible furnace during melting process.

3.2.3. Solidification of the alloy: after the melt is poured into the mould, various events occur during solidification and cooling to room temperature. These events have a great influence on the shape, size, uniformity and chemical composition of the grain developed throughout the casting, which in turn has a great influence on the overall properties. The crucial factors

affecting these events are type of metal, thermal properties of both metal and mould, the geometric relationship between the area and volume of the casting and the shape of the mould.

Figure 12. Produced alloy after melting and pouring.

3.2.4. Finishing process: The cast metal was then removed from the metal mould and placed in four different cooling media. The cooling media that were made use of include;

1. Natural/Ambient atmosphere (AIR)
2. Artificial atmosphere (FAN)
3. Spent engine oil
4. Ice block

After the cooling process, the projections left on the casting were removed with the use of a grinder, and also small sections were cut for both microstructural analysis and hardness testing.

Figure 13. NAB alloy cooling in air

Figure 14. NAB alloy cooling in artificial atmosphere (fan)

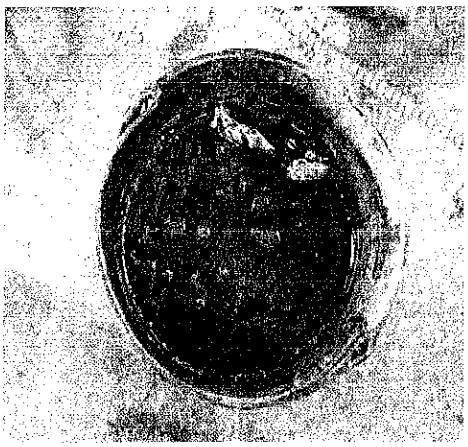

Figure 15. NAB alloy cooling in spent engine oil.

Figure 16. NAB alloy cooling in ice block

3.3 MICROSTRUCTURAL EXAMINATION

After the cooled NAB samples have been subjected to cooling in different media, microstructural examination is carried out on the samples using the optical microscope to analyze the microstructures of the developed alloy. The stages in the microstructural examination are;

3.3.1. Specimen preparation: The sample was cut into small sections which can easily be held in the hand. The specimen was obtained by cutting with a hacksaw or power saw.

3.3.2. Grinding and Polishing: Grinding involves preparation of the samples for microstructural analysis by making the surface scratch-free. The grinding was then carried out by holding the samples firmly against a motor-driven emery paper. The emery papers used were from a range of coarse grades to successively finer grades.

During grinding, flushing water was directed across the surface of the grinding papers which therefore served as a coolant.

The next stage of preparation (polishing) completely removed all the fine scratches and made the surface smooth and mirror-like. Polishing was carried out on a rotating cloth pad impregnated with a polishing medium (diamond paste). Then, the specimen was thoroughly washed in warm water.

Figure 17. Grinding machine

Figure 18. Polishing machine

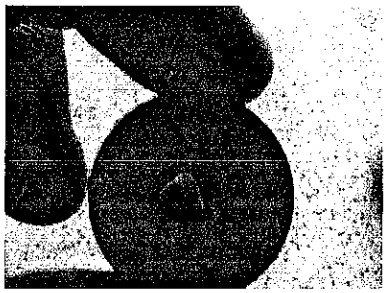

Figure 19. Polished sample

3.3.3. Etching: The polishing process, even if carefully carried out may leave a flawed layer on the surface of the specimen, which may have the effect of covering very fine cracks or included particles. Etching will remove this thin layer.

Etching was carried out by immersing the specimen in a suitable chemical reagent. The specimen was chemically etched by making use of swabbing technique. The etching reagent gradually dissolves the surface layer of the specimen and preferentially attacks the grain boundaries. The etchant used was acidified ferric chloride with HCl and water.

3.3.4. Microscopic analysis: The microscopic analysis was carried out with the aid of a computerized optical microscope attached with a digital photographic and data storage and retrieval system. Microscopic examination will reveal the microstructure of the alloy as well as the incidence of any porosity or cracks.

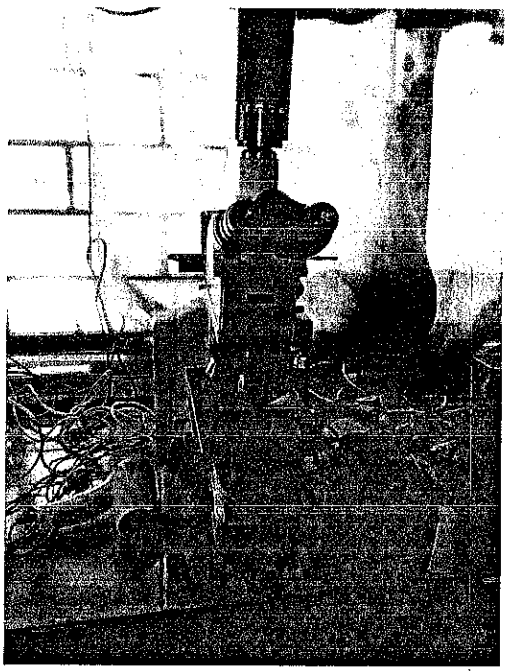

Figure 20. Optical metallurgical microscope

3.4 HARDNESS TEST

Hardness tests measure the resistance to penetration of the surface of a material by a hard object. The depth of penetration is measured by the testing machine. For the hardness test to be carried out successfully, the samples were grinded to a flat surface with the aid of a grinding machine.

The hardness tests were carried out on a digital Rockwell tester by applying a force of 60kgf (about 588N).

3.5 TENSILE TEST

The various NAB alloy samples were taken to the machining workshop, where it was cut and machined into the required specifications for tensile test analysis.

The equipment made use of was the Instron Universal Tester with a maximum load capacity of 50KN, which has a computerized interface.

The samples were put into the jaws of the tensile testing machine, and then it was stretched and stretched until it reached its breaking point (i.e it fractured).

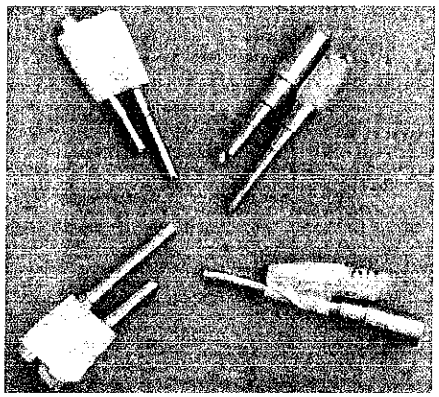

Figure 21: NAB alloy tensile specimens

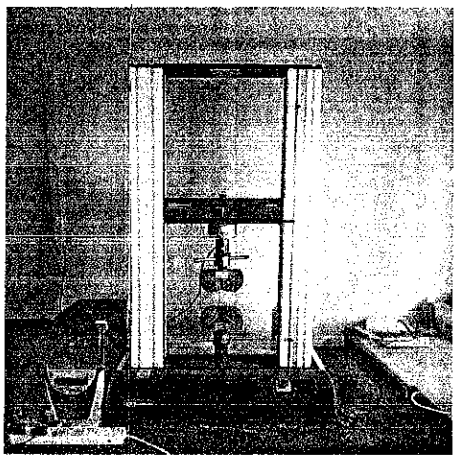

Figure 22. Instron Universal tester (50KN) equipped with tensile jaws

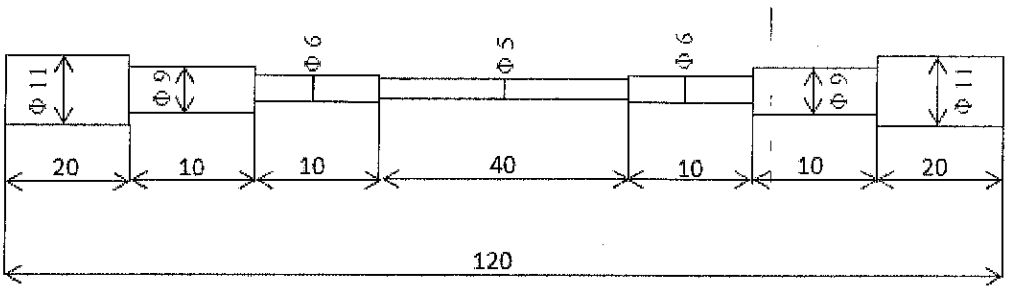

Figure 23. Dimensions of machined NAB sample

CHAPTER FOUR

4.0 EXPERIMENTAL RESULT AND DISCUSSION

4.1 CASTING

Sand casting was selected as the best means of casting NAB alloy based on its low cost, flexibility and availability of materials. The composition of the alloy (obtained by Spark test) is shown in the table below.

%C	**%Si**	**%Mn**	**%P**	**%S**	**%Cr**	**%Ni**	**%Sb**
>0.0072	**0.123**	**0.022**	**0.0077**	**0.10**	**0.0021**	**1.50**	**0.130**
%Al	**%Cu**	**%Co**	**%Ti**	**%Au**	**%B**	**%As**	**%Pb**
>6.32	**87.9**	**0.022**	**0.0030**	**0.018**	**0.0005**	**<0.025**	**0.416**
%Mg	**%B**	**%Sn**	**%Zn**	**%As**	**%Bi**	**%Cd**	**%Zr**
0.0036	**<0.0005**	**0.017**	**0.092**	**0.025**	**<0.0015**	**<0.0011**	**0.0000**
%Ln	**%Fe**						
<0.0035	**4.77**						

Table 3. Chemical composition of Nickel Aluminium Bronze (NAB) alloy after casting (wt%)

4.2. HARDNESS

The hardness result of the samples is plotted in a bar chart as a function of the cooled (air, fan, oil, ice) samples. The air-cooled sample has the lowest hardness compared to the other samples cooled in different mediums. The artificially cooled sample (i.e. with the use of a fan) attained the highest hardness.

The hardness of the samples was taken at different points on the samples and the average was taken and recorded.

COOLED SAMPLES	HARDNESS (HRA)			
	A	B	C	AVRG
AIR	85.7	85.9	84.4	85.3
FAN	87.7	86.7	87.1	87.2
ICE BLOCK	84.0	86.1	87.6	85.9
SPENT OIL	86.3	84.3	86.5	85.7

Table 4. Hardness of the cooled NAB alloys

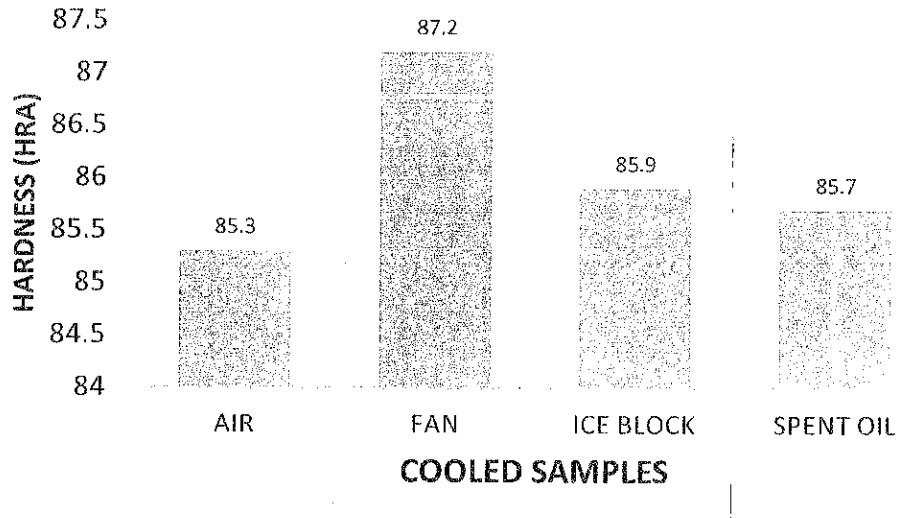

Figure 24. Typical mechanical (hardness) property of the cooled NAB samples.

4.3. TENSILE STRENGTH

The tensile strength values was determined from the stress-strain curve generated by the Instron universal tester.

The tensile strengths of the samples is plotted in a bar chart as a function of the cooled (air, fan, oil, ice) samples. The ice-cooled sample has the lowest hardness compared to the other samples cooled in different mediums. The sample cooled in spent engine oil attained the highest tensile strength.

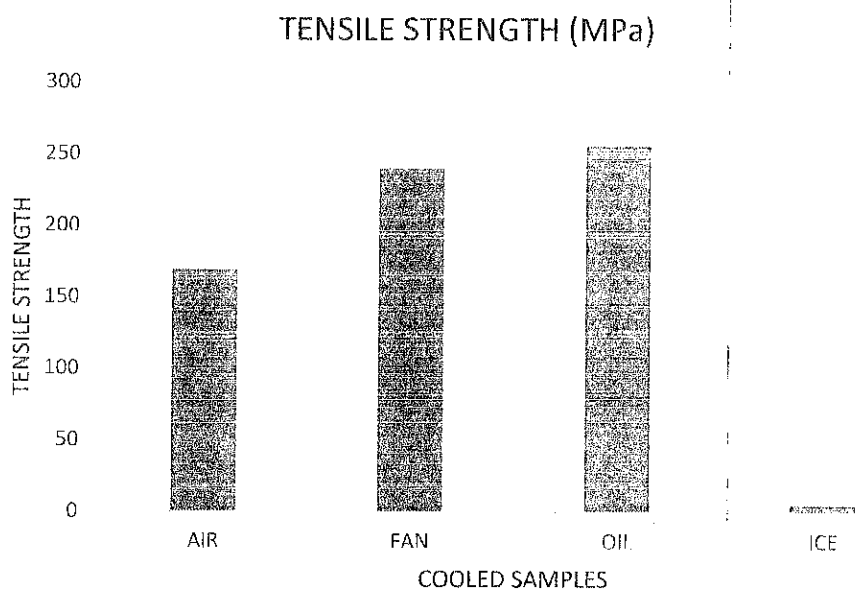

Figure 25. Typical mechanical (tensile strength) property of the cooled NAB samples.

4.4. MICROSTRUCTURE OF NICKEL ALUMINIUM BRONZE ALLOY

Plate 1: Microstructure of as-cast Nickel Aluminium Bronze (NAB) showing dendritic structure and different microstructures {primary α, eutectoid $\alpha + \gamma 2$ and Fe containing phases}. Etchant used – acidified ferric chloride with Hcl and water.

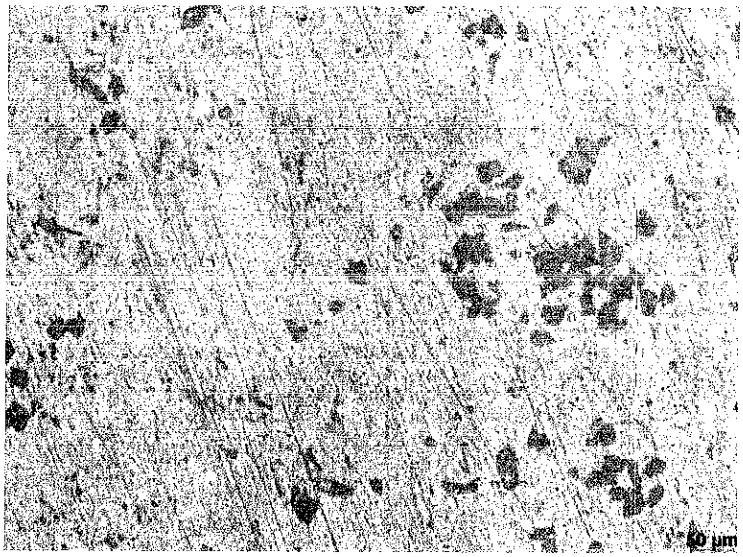

Plate 2: Microstructure of Nickel Aluminium Bronze (NAB) cooled with fan showing Fe rich phase with NiAl precipitates (tempered martensite). Etchant used – acidified ferric chloride with Hcl and water.

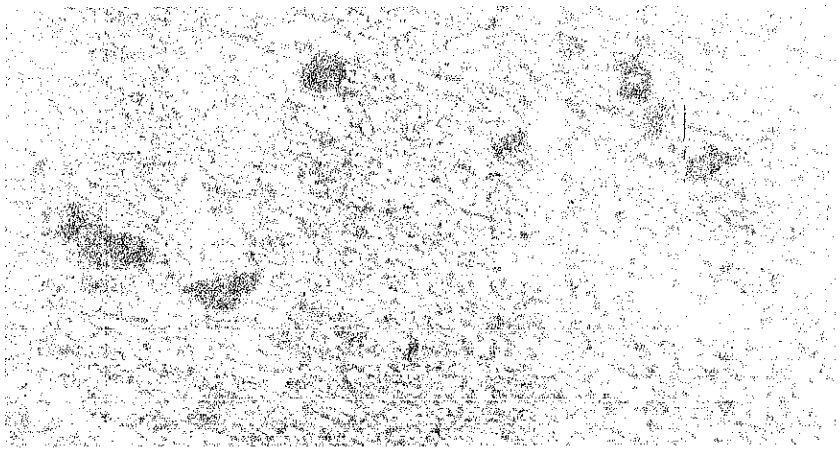

Plate 3: Microstructure of Nickel Aluminium Bronze (NAB) cooled with ice block showing precipitates of κ phases and α phases. Etchant used – acidified ferric chloride with Hcl and water.

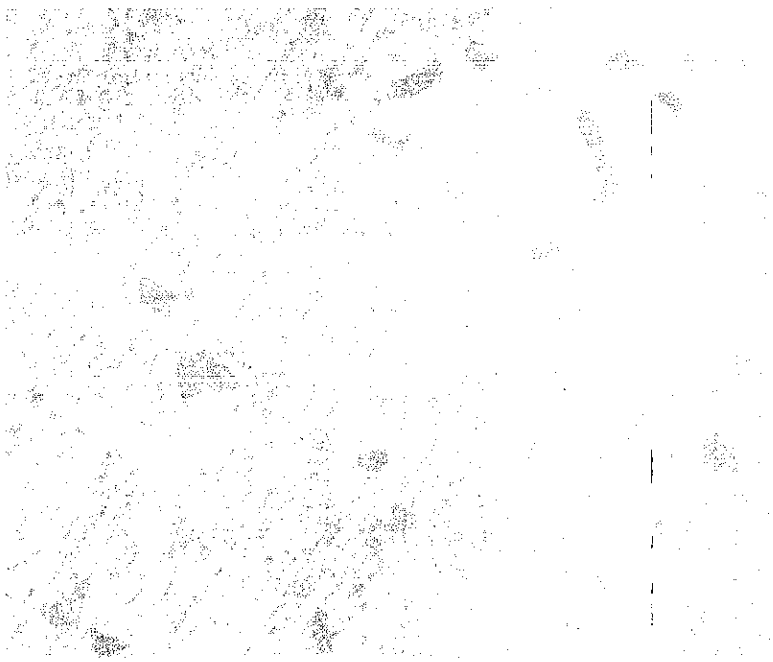

Plate 4: Microstructure of Nickel Aluminium Bronze (NAB) cooled in spent engine oil showing limited quantity of the eutectoid and primary α phase. Etchant used – acidified ferric chloride with Hcl and water.

4.5. DISCUSSIONS OF THE MICROSTRUCTURES

4.5.1 Microstructure of as-cast (air-sample) Nickel Aluminium Bronze alloy produced

The as-cast microstructure consists of copper-rich α phase, martensitic β′ and κ phases based on Fe_3Al. The precipitates have a dendritic morphology and are cored, the composition ranges from iron-rich solid solution to Fe_3Al.

The mode of distribution of different phases in the material system is shown. Needle like martensite and dark round particles may be seen. Other microconstituents like primary α surrounded by eutectoid ($\alpha + Ni_3Al$) along with Fe-rich phase.

4.5.2 Microstructure of artificially cooled (fan) NAB alloy produced

There is formation of fine Fe rich phase within the grains. However, during the cooling process, some of the high temperature β′ was retained as a martensitic structure and the martensite was then transformed into a very fine structure of α and κ phases, with NiAl precipitates, referred to as tempered martensite.

4.5.3. Microstructure of ice-cooled NAB alloy produced

There is transformation of β martensite into α and fine κ phases. It leads to the precipitation of a further κ phase which differs in chemical composition and morphology to those present in as-cast structure.

4.5.4. Microstructure of oil-cooled NAB alloy produced

This consists of α, β and κ phases. Martensite transformation occurred on β phase during cooling and the volume fraction of β′ increased due to the dissolution of α and κ phases.

CHAPTER FIVE

5.0. CONCLUSION AND RECOMMENDATION

5.1. CONCLUSION

This chapter presents conclusions arrived at based on the results obtained and observations made in this study. The conclusions relate to the microstructural alterations brought about by cooling in different media (air, fan, ice block, spent oil) and corresponding changes in mechanical properties such as hardness, tensile strength. The conclusions drawn from this study are listed below

1. The alloy displayed primary α, eutectoid $\alpha + \gamma 2$ as well as retained β' and martensite. The various cooling rates led to microstructural homogenization through the disappearance of the as-cast structure depending on the type of cooling medium employed.
2. Hardness of the samples improved after cooling in different media compared to the one in as-cast condition. The artificially cooled sample (with the use of a fan) attained the highest hardness amongst all, while the air-cooled sample attained the lowest hardness. The sample cooled with ice block has the second highest hardness.
3. The sample having the highest tensile strength is the sample cooled in spent engine oil.
4. The study suggests the microstructural features, hardness and tensile strength were affected by the rate of cooling. The cooling in various media (air, fan, ice, spent oil) also affected the characteristics of the sample to a considerable extent.

5.2. RECOMMENDATIONS

The following recommendations were suggested during the course of this project:

1. More facilities for research should be procured and installed in the departmental laboratory.
2. The effects of different alloying elements on Nickel Aluminium Bronze (NAB) alloy should be studied.
3. Deep investigations should be carried out in order to know the necessary steps to take to achieve the aim of the study.

REFERENCES

Ajeel, S.A., Ibraheim, S.N., Salam, A., Fadhil, A. Engineering and Technology, Vol. 25, 2007, p. 711-727.

American Society for Testing and Materials (ASTM) E-8, Standard Test Methods for Tension Testing of Metallic Materials.

ASTM B148-97(2003), Standard specification for Aluminium Bronze Sand Castings, ASTM

Anantapong, J.; Uthaisangsuk, V.; Suranuntchai, S.; Manonukul, A. Effect of hot working on microstructure evolution of as-cast Nickel Aluminum Bronze alloy. *Mater. Des.* **2014**, *60*, 233–243.

A Schussler and H. E. Exner, "The Corrosion of Nickel-Aluminium Bronzes in Seawater -I.Protective Layer Formation and the Passivation Mechanism," *Corrosion Science*, Vol. 34, 1993, p. 1793.

Callcut, V.A: Metals and Materials, Vol. 5 (3), 1989, p. 128-132.

Chen, R-p., Liang, Z-q., Zhang, W-w, Zhang, D-t., Luo, Z-q., Li, Y-y, *Effect of heat treatment on microstructure and properties of hot-extruded nickel-aluminium bronze,* Transactions of Nonferrous Metals Society of China 17(2007), 1254-1258.

Culpan, E.A and Rose R., "Corrosion Behaviour of Cast Nickel Aluminum Bronze in Sea Water," *British Corro-sion Journal*, Vol. 14, No. 3, 1979, p. 160.

Dawson, R.J.C: Engineering Materials and Design, Vol. 22 (12), 1978, p. 25-28.

Fuller, M.D., Swaminathan, S., Zhilyaev, A.P., and Mcnelley, T.R. "Microstructural Transformations and Mechanical Properties of Cast NiAl Bronze: Effects of Fusion Welding and Friction Stir Processing," *Materials Science and Engineering A*, Vol. 463

Gao, L.L.; Cheng, X.H. Microstructure and mechanical properties of Cu–10%Al–4%Fe alloy produced by equal channel angular extrusion. *Mater. Des.* **2008**, *29*, 904–908.

Hanke, S.; Fischer, A.; Beyer, M.; Santos, J.D. Cavitation erosion of NiAl-bronze layers generated by friction surfacing. *Wear* **2011**, *273*, 32–37.

Hasan, F., Iqbal, J., and Ridley, N., "*Materials Science Technology*, Vol. 1, 1985, p. 312.

Hasan, F., Jahanafrooz, A., Lorimer, G.W., Ridley, N., "The Morphology, Crystallography, and Chemistry of Phases in As-Cast Nickel-Aluminum Bronze," *Met. Trans A,* v.13a, p.1337-1345, 1982.

Hasan, F., Lorimer, G.W., Ridley, N., "Crystallography of Martensite in a Cu-10Al-5Ni-5Fe alloy," Journal de Physique, v.43, p.C4 653-C4 658, 1982.

Jahanafrooz, A.; Hasan, F.; Lorrmer, G.W.; Ridley, N. Microstructural development in complex nickel aluminum bronzes. *Metall. Mater. Trans. A* 1982, *14*, 1951–1956.

Lenard, D.R.; Bayley, C.J. Electrochemical monitoring of selective phase corrosion of NiAl bronze in Seawater. *Corrosion* **2008**, *64*, 764–772.

Mahoney, Murray W., Bingel, William H., Mishra, Rajiv S., *Materials Science Forum*, v. 426-432, p. 2843-2848, 2003

Mcnelley, T.R. Peak Stir Zone Temperatures during Friction Stir Processing. *Metall. Mater. Trans. A* **2009**, *41*, 631–640.

Mishra, R.S., Ma, Z.Y., "Friction Stir Welding and Processing," *Materials Science and Engineering*, v. 50, p. 1-78, 2005.

Nandan, R.; Debroy, T.; Bhadeshia, H. Recent advances in friction stir welding process, weldment structure and properties. *Prog. Mater. Sci.* **2008**, *53*, 980–1023.

Nelson, E.A: Microstructural effects of multiple passes during friction stir processing of nickel

aluminium bronze, Thesis at Naval Postgraduate School, Monterey, California, December 2009.

Ni, D.R.; Xiao, B.L.; Ma, Z.Y.; Qiao, Y.X.; Zheng, Y.G. Corrosion properties of friction stir processed cast NiAl bronze. *Corros. Sci.* **2010**, *52*, 1610–1617.

Oh-Ishi, K. and McNelley, T., "The Influence of Friction Stir Processing Parameters on Microstructure of As-Cast NiAl Bronze" *Metallurgical and Materials Transactions, v.* 36A, p. 1575-1585, 2005.

Robert, J.F., and Thomas, E.C. Material Performance, Vol. 431, 1982, pp. 30-34

Sahoo, M., "Structure and Mechanical Properties of Slow-Cooled Nickel Aluminum Bronze Alloy C95800," *AFS Trans,* v. 90, p. 913-926, 1982.

Shan, D.B., Wang, Z., Lu, Y., Xue, K.M: J. Mater. Proc. Tech., 72, 1997, p. 403-406

Song, Q.N.; Zheng, Y.G.; Ni, D.R.; Ma, Z.Y. Studies of the nobility of phases using scanning Kelvin probe microscopy and its relationship to corrosion behaviour of Ni–Al bronze in chloride media. *Corro. Sci.* **2014**, *92*, 95–103.

Su, J.; Swaminthan, S.; Menon, S.K.; Mcnelley, T.R. The effect of concurrent straining on phase transformations in NiAl bronze during the friction stir processing thermomechanical Cycle. *Metall. Mater. Trans. A* **2011**, *42*, 2420–2430.

Tang, C.H.; Cheng, F.T.; Man, H.C. Effect of laser surface melting on the corrosion and cavitation erosion behaviors of a manganese–nickel–aluminium bronze. *Mater. Sci. Eng. A* **2004**, *373*, 195–203.

Thuanboon, S: Development of nickel aluminum bronze casting for ship propeller, Report of Royal Thai Naval Dockyard. 2010.

Wenschot, P., "The Properties of Ni-Al Bronze Sand Cast Ship Propellers in

Relation to Section Thickness," *International Shipbuilding Progress,* v. 34, p.112-123, 1987.

Weronski, W and Gontarz, A: J. Mater. Proc. Tech., 138, 2003, p. 196-200.

Wharton, J.A., Barik, R.C., Kear, G., Wood, R. J. K., Stokes, K. R., Walsh, F. C., 2005, 'The Corrosion of Nickel-aluminium Bronze in Seawater', *Corrosion Science 47 (2005) 3336-3367,* Elsevier.

Wharton, J.A.; Stokes, K.R. The influence of nickel–aluminium bronze microstructure and crevice solution on the initiation of crevice corrosion. *Electrochim. Acta* **2008**, *53*, 2463–2473

http://properties.copper.org/.

http://www.copper.org